pISSN 1598-2998, eISSN 2005-9256
https://doi.org/10.4143/crt.2020.694
Cancer Res Treat. 2021;53(2):389-398

Original Article

Clinical and Genomic Characteristics of Adult Diffuse Midline Glioma

Changhee Park[1], **Tae Min Kim**[1,2], **Jeong Mo Bae**[3], **Hongseok Yun**[4], **Jin Wook Kim**[5], **Seung Hong Choi**[6], **Soon-Tae Lee**[7], **Joo Ho Lee**[8], **Sung-Hye Park**[3], **Chul-Kee Park**[5]

[1]Department of Internal Medicine, Seoul National University Hospital, Seoul, [2]Cancer Research Institute, Seoul National University, Seoul, [3]Department of Pathology, Seoul National University Hospital, Seoul, [4]Biomedical Research Institute, Seoul National University Hospital, Seoul, Departments of [5]Neurosurgery, [6]Radiology, [7]Neurology, and [8]Radiation Oncology, Seoul National University Hospital, Seoul, Korea

Purpose The treatment outcomes and genomic profiles of diffuse midline glioma (DMG) in adult patients are rarely characterized. We performed a retrospective study to evaluate the clinicogenomic profiles of adult patients with brain DMG.

Materials and Methods Patients aged ≥ 18 years diagnosed with brain DMG at Seoul National University Hospital were included. The clinicopathological parameters, treatment outcomes, survival, and genomic profiles using 82-gene targeted next-generation sequencing (NGS) were analyzed. The 6-month progression-free survival (PFS6) after radiotherapy and overall survival (OS) were evaluated.

Results Thirty-three patients with *H3*-mutant brain DMG were identified. The median OS from diagnosis was 21.8 months (95% confidence interval [CI], 13.2 to not available [NA]) and involvement of the ponto-medullary area tended to have poor OS (median OS, 20.4 months [95% CI, 9.3 to NA] vs. 43.6 months [95% CI, 18.2 to NA]; p=0.07). Twenty-four patients (72.7%) received radiotherapy with or without temozolomide. The PFS6 rate was 83.3% (n=20). Patients without progression at 6 months showed significantly prolonged OS compared with those with progression at 6 months (median OS, 24.9 months [95% CI, 20.4 to NA] vs. 10.8 months [95% CI, 4.0 to NA]; p=0.02, respectively). Targeted NGS was performed in 13 patients with DMG, among whom nine (69.2%) harbored concurrent *TP53* mutation. Two patients (DMG14 and DMG23) with *PIK3CA*$^{R38S+E545K}$ and *KRAS*^{G12A} mutations received matched therapies. Patient DMG14 received sirolimus with a PFS of 8.4 months.

Conclusion PFS6 after radiotherapy was associated with prolonged survival in adult patients with DMG. Genome-based matched therapy may be an encouraging approach for progressive adult patients with DMG.

Key words Diffuse midline glioma, Concurrent chemoradiotherapy, Targeted sequencing

Introduction

In the 2016 World Health Organization (WHO) classification, histone 3 (*H3*) K27M-mutant diffuse midline glioma (DMG) was recognized as a distinct entity among high-grade gliomas [1]. DMG accounts for approximately 20% of pediatric glioblastomas, and its clinical characteristics have been described in detail in previous studies [2]. The midline locations of DMG tumors at presentation impede complete tumor removal, resulting in a poor survival outcome. Additionally, a previous study reported that *H3* K27M-mutant DMG showed poorer survival than other grade IV gliomas that arose at the midline in a pediatric population [3]. However, growing understanding of the biology and descriptions of the outcomes of *H3* K27M-mutant DMG is contributing to improvement of treatment outcomes.

DMGs are notable for harboring histone mutations, including *H3F3A* K27M, *H3F3A* G34R, and *H3F3A* G34V [4,5]. Genomic characterization of DMG in pediatric populations showed a high incidence of concurrent *TP53* mutations and alterations in growth factor pathways [5]. In younger children in a mean age of 3 years with DMG, the *ACVR1* somatic gain-of-function mutation was mainly found, resulting in the hyperactivation of bone morphogenetic protein signaling and ventralization of zebrafish embryos [6]. Additionally, genes involved in the phosphatidylinositol-3 kinase (PI3K) pathway were also altered. These genomic profiles facilitate the prognostications as well as precision treatment decisions of patients with DMG.

DMG is also found in adult patients with similar clinical features to those of pediatric patients [7,8]. However, because of its relatively rare incidence compared with pediatric populations, a comprehensive description encompassing clinical features and genomic profiles of adult DMG is still lacking. Furthermore, the clinical outcomes of palliative treatments for recurrent or refractory DMG have been scarcely described. Although precision medicine-guided treatment improved therapy recommendations using genomic and transcriptional profiling in advanced common cancers [9], precision medicine trials have been limited in rare cancers such as DMG.

Correspondence: Tae Min Kim
Department of Internal Medicine, Seoul National University Hospital, 101 Daehak-ro, Jongno-gu, Seoul 03080, Korea
Tel: 82-2-2072-3559 Fax: 82-2-2072-3559 E-mail: gabriel9@snu.ac.kr
Received August 19, 2020 **Accepted** November 6, 2020 **Published Online** November 9, 2020

In this study, we described the clinical outcomes of adult patients with DMG and their genomic profiles through a retrospective analysis of 33 adult patients with DMG.

Materials and Methods

1. Patients and histology

We searched records for adult patients aged ≥ 18 years who were diagnosed with DMG involving the brain at Seoul National University Hospital between May 2005 and September 2019. DMG was defined as an infiltrative midline high-grade glioma with predominantly astrocytic differentiation and *H3F3A* or *HIST1H3B*/C mutation according to the 2016 WHO classification [1] by experienced pathologists (J.M.B. and S.-H.P). *H3F3A* K27M or G34V mutation was confirmed by the detection of K27M-mutant protein using an anti-histone H3.3 antibody (ABE419, Millipore, Temecula, CA) or targeted next-generation sequencing (NGS). Patients with an inconclusive diagnosis were excluded. The details on other histologic diagnosis methods including probes for immunohistochemistry (IHC) and fluorescent *in situ* hybridization are provided at Supplementary Methods.

Data including the patients' demographics, radiographic findings, pathologic findings, diagnosis date, detailed treatments, initiation date of treatments, status of disease progression, and survival outcomes, were collected using the electronic medical records system.

2. Definition of clinical parameters and treatments

The surgical extent of DMG was classified into four groups based on the following: gross total resection (GTR) as complete resection of the mass and no visualized enhanced signal intensity in contrast-enhanced brain magnetic resonance imaging (MRI) obtained within 48 hours after surgery; near-total resection visualized as thin enhanced signal intensity in contrast-enhanced brain MRI obtained within 48 hours after surgery; subtotal resection as grossly remained tumor or visualized nodular enhancement in contrast-enhanced brain MRI obtained within 48 hours; biopsy only as biopsy without intent to tumor resection. We additionally evaluated T2 fluid attenuated inversion recovery (FLAIR) images to determine if there were any possible findings of residual tumors that were not identified by contrast-enhanced images.

The protocol used for concurrent chemoradiotherapy (CCRT) with temozolomide (TMZ) was either a standard 6-week [10] or hypofractionated 3-week interval based on age (≥ 70 years) or poor performance status [11]. The objective responses to radiotherapy with or without TMZ and palliative systemic treatments were evaluated according to the revised Response Assessment in Neuro-Oncology criteria [12]. Additionally, progression-free survival (PFS) was defined as the time to progression or death from treatment initiation and overall survival (OS) was defined as the time to death from diagnosis. We evaluated the association of the 6-month progression-free survival (PFS6) from radiotherapy initiation, a commonly used endpoint in glioblastoma, with the OS from diagnosis [13].

3. Targeted NGS profiles for adult DMG

Thirteen patients with available targeted NGS results were included. Genomic DNA was extracted from formalin-fixed paraffin-embedded tissue and was fragmented using a Covaris sonicator (Covaris, Woburn, MA). Agilent's SureSelectXT Custom protocol was used to construct libraries (Agilent Technology, Santa Clara, CA), and MiSeqDx or NextSeq 550Dx (Illumina Inc., San Diego, CA) was used for sequencing.

The produced sequencing data were analyzed using the SNUH First Panel Analysis Pipeline. We performed quality control of the FASTQ file and further analyzed only the data that passed the criteria. Pair-end alignment to the hg19 reference genome was performed using BWA-men (v0.7.17) and GATK Best Practice [14,15].

After finishing the alignment step, an "analysis-ready BAM" was produced, and variants such as single-nucleotide variant (SNV), InDel, copy number variation (CNV), and translocation were detected using at least more than two analysis tools, including SNUH in-house and open-source software. GATK UnifiedGenotyper (v4.0.6.0), SNVer (v0.5.3), and LoFreq (v2.1.0) were used for SNV/InDel detection [15,16]; Delly (v0.7.8) and Manta (v1.4.0) for translocation discovery [17,18]; and THetA2 (v0.7) and CNVKit (v0.9.3) for purity estimation and CNV calling [19,20].

From those, we retained the variants meeting the following requirements: variant allele frequency ≥ 5%, reads supporting for alternative allele ≥ 10, reads supporting for alternative allele ≥ 10, and reads supporting each strand for alternative allele > 5 for SNV/InDel; copy number ≥ 6 and copy number ≤ 1 for CNV; split-reads supporting for alternative allele ≥ 10 for translocation. Other filtering criteria were applied using the default parameters of the analysis tools.

The detected variants were annotated by SnpEff (v4.3) using various databases such as RefSeq, COSMIC (v84), dbSNP (build 150), ClinVar (2018-06), and gnomAD (v2.0.1). The germline variant was filtered using the population frequency of these databases (> 1% population frequency) [21-26]. Finally, the variants were confirmed throughout a comprehensive review of a multidisciplinary molecular tumor board. The list of genes assessed by targeted NGS is provided in S1 Table.

Table 1. Patient demographics

Characteristic	No. (%) (n=33)
Age at diagnosis, median (range, yr)	39 (20-70)
Sex	
Male	17 (51.5)
Female	16 (48.5)
Initial symptoms	
Dizziness	9 (27.3)
Memory impairment	9 (27.3)
Headache	8 (24.2)
Diplopia	6 (18.2)
Gait abnormality	5 (15.2)
Abnormal odor sensation	3 (9.1)
Dysarthria	3 (9.1)
Motor weakness	3 (9.1)
Visual field defect	3 (9.1)
Others[a)]	10 (30.3)
Ponto-medullary involvement	
Yes	14 (42.4)
No	19 (57.6)
Initial KPS	
100	3 (9.1)
80-90	16 (48.5)
50-70	10 (30.3)
Initial surgery extent	
Biopsy only	19 (57.6)
Subtotal resection	8 (24.2)
Near-total resection	3 (9.1)
Gross total resection	3 (9.1)
Radiotherapy	
CCRT with TMZ	20 (60.1)
Radiotherapy alone	4 (12.1)
Gamma-knife surgery	1 (3.0)
Subsequent treatment after progression from initial treatment	
Surgery	4 (12.1)
Gamma-knife surgery	1 (3.0)
Systemic chemotherapy	11 (33.3)
Radiotherapy	2 (6.1)
CCRT	1 (3.0)
Histologic-genomic findings	
ATRX mutation	10 (32.2)
IDH1 mutation	1 (3.0)
CDKN2A deletion	6 (26.1)
PTEN loss	8 (34.8)
MGMT promotor methylation	1 (3.0)

CCRT, concurrent chemoradiotherapy; KPS, Karnofsky performance status; TMZ, temozolomide. [a)]Other initial symptoms include facial palsy (n=2), loss of consciousness (n=2), swallowing abnormality (n=2), sensory abnormality (n=2), dysphasia (n=1), and tinnitus (n=1).

4. Statistical analysis

Descriptive statistics were mainly used to demonstrate the results in this study. To describe and compare the survival outcome, Kaplan-Meier survival curves and log-rank survival analysis were used. Cox proportional hazard model for univariate analysis was used to determine clinical factors associated with OS in patients who received radiotherapy. Next, Cox proportional hazard model for multivariate analysis was used with age, gender and the factors with p-values less than 0.2. Logistic regression analysis was performed to evaluate whether a genomic alteration identified at least two samples by NGS affects PFS6 in patients who received CCRT. Ninety-five percent confidence intervals (CI) were calculated for survival analyses. Fisher exact test was used to compare categorical values. p-values less than 0.05 were considered as statistically significant. All statistical analyses were performed using R software ver. 3.5.1 (https://www.r-project.org).

Results

1. Patients and histologic findings

The demographics and histologic findings of patients with DMG are summarized in Table 1. Thirty-four adult patients were searched via an electronic medical record system, and 33 were confirmed to have *H3*-mutant DMG. One patient with an inconclusive diagnosis was excluded because of insufficient tumor tissue available for assessment. Thirty-two patients were confirmed by IHC, and one with *H3F3A* G34V mutation (S2 Fig.) was confirmed by targeted NGS. All the patients had lesions at the midline of the brain including the basal ganglia, thalamus, midbrain, pons, and medulla. All the patients had neurologic symptoms related to the lesion at the time of the first diagnosis. Dizziness and memory impairment were the most common symptoms (n=9, 27.3%, respectively).

IHC detected *ATRX* mutant protein in 10 of 31 patients (32.2%). *IDH1*-mutant protein was observed in only one patient. *IDH2* mutation was not observed. *CDKN2A* deletion and *PTEN* loss by fluorescence *in situ* hybridization were observed in six of 23 (26.1%) and eight of 23 (34.8%) patients, respectively. O^6-methylguanine-DNA methyltransferase (*MGMT*) promoter methylation was observed in one patient.

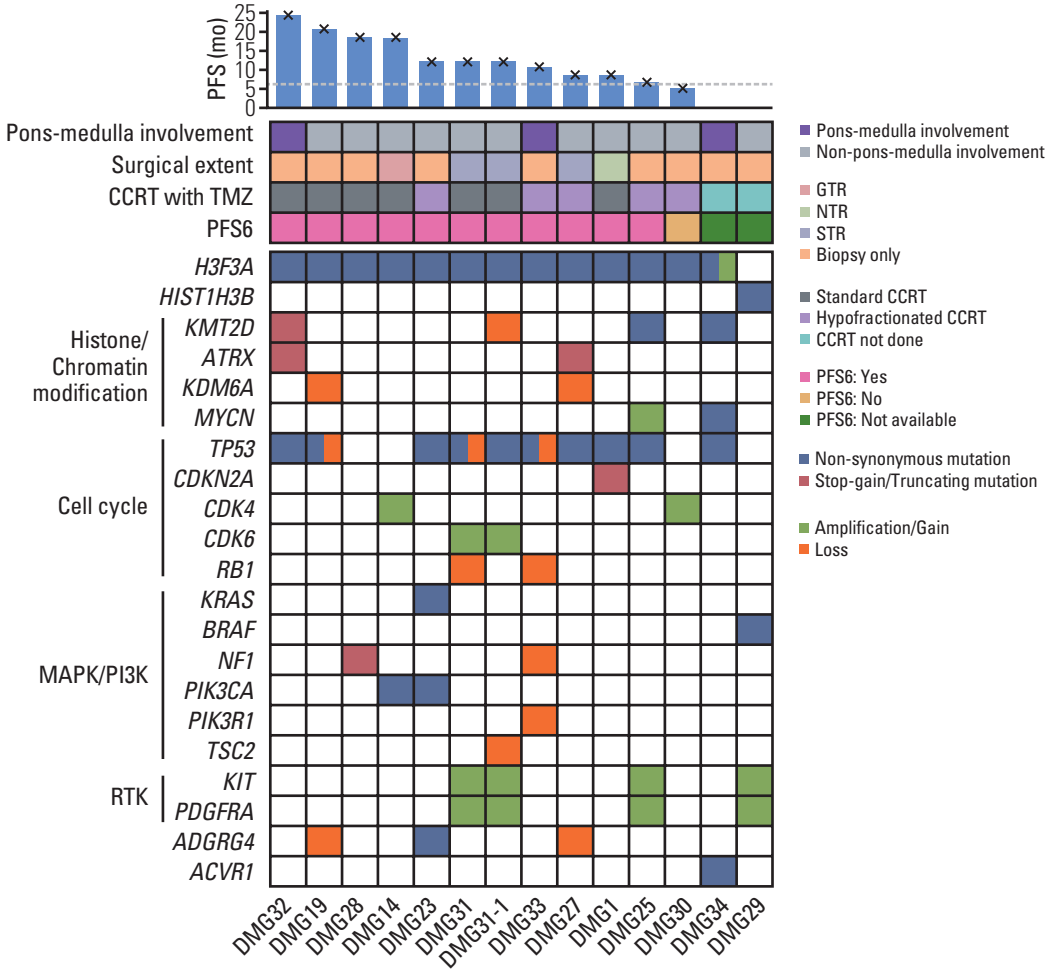

Fig. 1. Genomic landscape of adult patients with DMG obtained by targeted NGS. The landscape plot shows the genomic landscape of adult patients with DMG obtained by targeted NGS. The annotations with corresponding colors are described at the bottom. At the top of the plot, the bar plot shows the PFS of CCRT with TMZ of each patient with a cross mark depicting events. The dashed line crosses y-axis at 6 months. Below the bar plot is a tile plot that depicts the clinical features of each patient. The numbers at the bottom of the plots are the index numbers of the patients. Paired NGS samples at the time of diagnosis and progression after CCRT with TMZ were obtained from patient DMG31 (samples DMG31 and DMG31-1). CCRT, concurrent chemoradiotherapy; DMG, diffuse midline glioma; GTR, gross total resection; MAPK, mitogen-activated protein kinase; NGS, next-generation sequencing; NTR, near-total resection; PFS, progression-free survival; PFS6, 6-month progression-free survival; PI3K, phosphatidylinositol-3 kinase; RTK, receptor tyrosine kinase; STR, subtotal resection; TMZ, temozolomide.

2. Genomic features of adult patients with DMG by targeted NGS

Thirteen patients had available targeted NGS data with a median tumor fraction of 85% (range, 20% to 90%) and a median average read depth of 1,016.3 (range, 649.7 to 2,066.5). All patients had *H3* K27M mutation, among whom 12 had mutations at *H3F3A* and one had mutation at *HIST1H3B*. One patient had amplification of *H3F3A*. *TP53* mutation was the most commonly altered gene (n=9, 69.2%). Eleven samples harbored alteration in cell cycle genes, including *TP53*, *CDKN2A*, CDK4, *CDK6*, and *RB1*. Alterations in mitogen-activated protein kinase (MAPK)/PI3K pathways, including *KRAS*, *BRAF*, *NF1*, *PIK3CA*, and *PIK3R1*, were observed in five patients (38.5%). Receptor tyrosine kinase amplification involving *KIT* and/or *PDGFRA* was observed in three patients (23.1%). *ACVR1* and *ATRX* gene alterations were observed in one and two patients, respectively. *IDH1* and *IDH2* mutations were not observed in these 13 patients. None of the 13 patients had *CDKN2A* deletion or *PTEN* loss by targeted NGS. Structural variant was not identified in

Table 2. Mutational profiles of adult patients with DMG

	Targeted NGS results of this study (n=13)	Schwartzentruber et al. [5] (n=15)	Mackay et al. [4] (n=200)	Nikbakht et al. [27] (n=9)	Aihara et al. [7] (n=7)
Population	Adult	Pediatric	Pediatric	Pediatric	Adult
ATRX	2 (15.4)	9 (60.0)	46 (23.0)	3 (33.3)	2 (28.6)
ACVR1	1 (7.7)	0	28 (14.0)	3 (33.3)	NA
BRAF	1 (7.7)	0	1 (0.5)	NA	0
NF1	2 (23.1)	3 (20.0)	11 (5.5)	NA	3 (42.9)
PDGFRA	0	3 (20.0)	21 (10.5)	0	0
PIK3CA	2 (15.4)	0	23 (11.5)	3 (33.3)	0
TP53	9 (69.2)	12 (80.0)	126 (63.0)	5 (55.6)	2 (28.6)

Values are presented as number (%). DMG, diffuse midline glioma; NA, not available; NGS, next-generation sequencing.

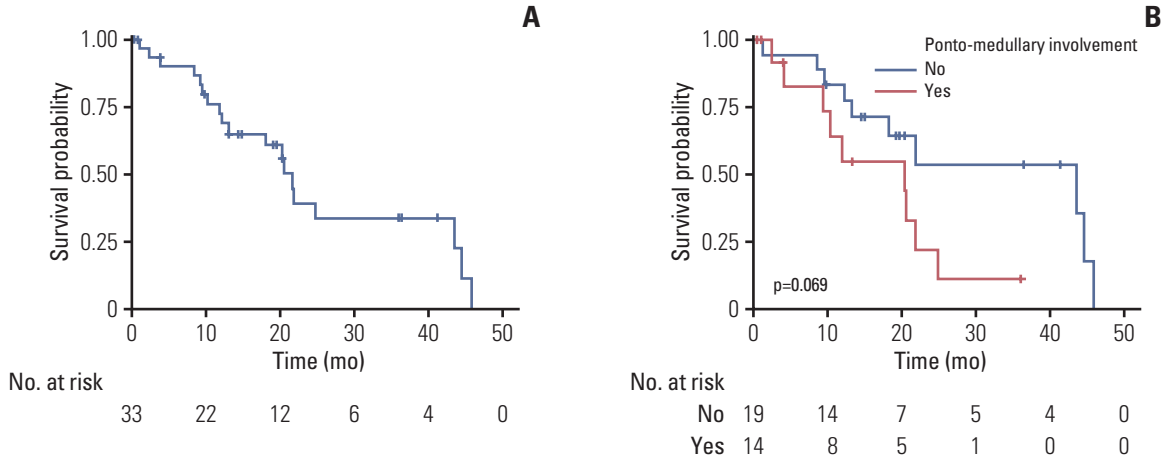

Fig. 2. Kaplan-Meier curves for the OS from diagnosis of all patients with DMG patients included in the study. (A) The Kaplan-Meier curve shows the overall survival of all patients with DMG. (B) The Kaplan-Meier curves show the overall survival of all patients with DMG according to ponto-medullary involvement. The blue line represents patients without ponto-medullary involvement; the red line represents patients with ponto-medullary involvement. The risk tables are below each plot, and p-values by the log-rank test are annotated in each plot. Censored data are depicted by vertical marks. DMG, diffuse midline glioma; OS, overall survival.

these patients. The genomic features of patients in this study are demonstrated in Fig. 1 (Detailed results are provided in S3 and S4 Tables).

One patient (DMG31) had paired targeted NGS data at the times of the first resection and re-surgery for relapsed tumor after adjuvant *CCRT* with *TMZ* (PFS of 13.3 months after the first resection). Although the latter sample harbored additional mutations in *JUN* and *MAPK3*, and loss of *TSC2* (Fig. 1, S3 and S4 Tables), both samples showed similar genomic profiles with mutations in *H3F3A* and *TP53* and amplifications in *KIT*, *PDGFRA*, and *CDK6*.

Comparisons with published mutational profiles are summarized in Table 2 [4,5,7,27]. *TP53* mutations were frequently observed throughout the studies. *ATRX* and *ACVR1* mutations were observed less commonly in our study than in other studies. Mutations in the MAPK/PI3K pathway were observed in few samples.

3. Survival outcomes of adult patients with DMG

The median OS from diagnosis was 21.8 months (95% CI, 13.2 to NA) (Fig. 2A), and 14 patients with involvement of the ponto-medullary area tended to have poor OS compared with 19 patients without involvement of the ponto-medullary area (median OS, 20.4 months [95% CI, 9.3 to not available (NA)] with involvement vs. 43.6 months [95% CI, 18.2 to NA] without involvement; p=0.07) (Fig. 2B). The 1-year and 3-year survival rates were 72.3% (95% CI, 57.6 to 90.7) and 33.4% (95% CI, 8.1 to 61.0), respectively.

Fourteen patients (42.4%) underwent surgical resection of tumors for initial treatment. While only three of 14 patients

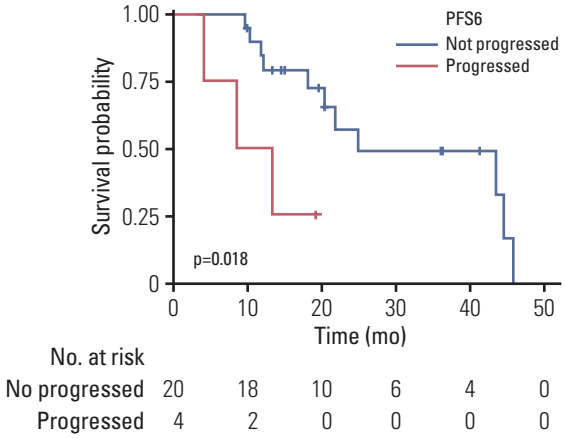

Fig. 3. Kaplan-Meier survival curves for the OS from diagnosis of patients according to PFS6 status from radiotherapy. The Kaplan-Meier curves show the OS from diagnosis of patients who received radiotherapy. The blue line represents patients without progression at 6 months after radiotherapy initiation; the red line represents patients whose diseases had progressed at 6 months. The risk tables are below each plot, and p-values by the log-rank test are annotated in each plot. Censored data are depicted by vertical marks. OS, overall survival; PFS6, 6-month progression-free survival.

(21.4%) with ponto-medullary involvement underwent surgical resection, 11 of 19 patients (57.9%) without ponto-medullary involvement underwent surgical resection including three GTR cases. Surgical resection was not associated with prolonged OS in all patients (median OS, 21.9 months [95% CI, 13.2 to NA] for the resected group vs. 20.4 months [95% CI, 11.9 to NA] for the unresected group; p=0.84) (S5A Fig.). Additionally, GTR did not prolong the survival after surgery compared with non-GTR in patients who had undergone surgical resection (median PFS, 8.0 months [95% CI, 4.2 to NA] vs. 11.9 months [95% CI, 9.6 to NA]; p=0.40 [S5B Fig.] and median OS, 13.2 months [95% CI, 9.6 to NA] vs. 21.9 months [95% CI, 21.8 to NA]; p=0.60 [S5C Fig.]). Furthermore, one patient who achieved GTR and had no residual T2-high signal by T2 FLAIR images showed PFS after surgery of 19.4 months, which is the longest survival among the patients who achieved GTR.

Twenty-four patients received radiotherapy: 20 and four patients received CCRT with TMZ and radiotherapy alone, respectively. Except for three patients who had received adjuvant chemoradiotherapy after GTR, the objective response rate of radiotherapy was 28.6% (n=6). The median PFS was 9.7 months (95% CI, 8.4 to 15.8), and the median OS was 24.9 months (95% CI, 18.2 to NA). The PFS6 rate was 83.3% (n=20; 95% CI, 69.7 to 99.7), and those without progression at 6 months showed significantly prolonged OS compared with the other four patients with progression at 6 months (median OS, 24.9 months [95% CI, 20.4 to NA] vs. 10.8 months [95% CI, 4.0 to NA]; p=0.02) (Fig. 3). The association of PFS6 and OS was consistent in multivariate analysis (hazard ratio, 0.12 [95% CI, 0.02 to 0.65]; p=0.01) (S6 Table). Comparisons of the treatment outcomes compared with other studies are summarized in Table 3 [8,28]. Tumor resection did not prolong PFS after radiotherapy (p=0.26) (S7A Fig.) and OS (p=0.61) (S7B Fig.). Additionally, GTR was not associated with prolonged PFS after radiotherapy in patients who had undergone resection (p=0.64) (S7C Fig.).

ATRX mutation was not associated with PFS compared with *ATRX* wild type (median PFS, 11.4 months [95% CI, 6.8 to NA] vs. 10.7 months [95% CI, 8.4 to 18.4]; p=0.86). Neither *CDKN2A* deletion nor *PTEN* loss was associated with PFS (p=0.41 and p=0.22, respectively). Additionally, *ATRX* mutation, *CDKN2A* deletion; and *PTEN* loss were not associated with OS in the patients who had received CCRT with TMZ (p=0.74, p=0.93, and p=0.84, respectively). In addition,

Table 3. Comparisons of adult patients with DMG with those in previous studies

	This study (n=33)	Meyronet et al. [8] (n=21)	Schreck et al. [28] (n=18)
Age (yr)	20-70	18-82	30-68
IDH1/2 mutation, n (%)	1 (3.0)	0	0
MGMT promoter methylation, n (%)	1 (3.0)	1 (4.8)	1 (5.6)
Resection rate (GTR rate) (%)	42.4 (9.1)	19.0 (NA)	28 (6)
Patients who received CCRT or RT (%)	72.7	66.7	65.0
ORR (%)	27.2	NA	NA
Median OS from diagnosis in all patients (mo)	21.8	19.6	17.6
Median OS from diagnosis in patients who received CCRT or RT (mo)	24.9	25.0	NA

CCRT, concurrent chemoradiotherapy; DMG, diffuse midline glioma; GTR, gross total resection; IDH, isocitrate dehydrogenase; MGMT, O^6-methylguanine-DNA methyltransferase; NA, not available; ORR, overall response rate; OS, overall survival; RT, radiotherapy.

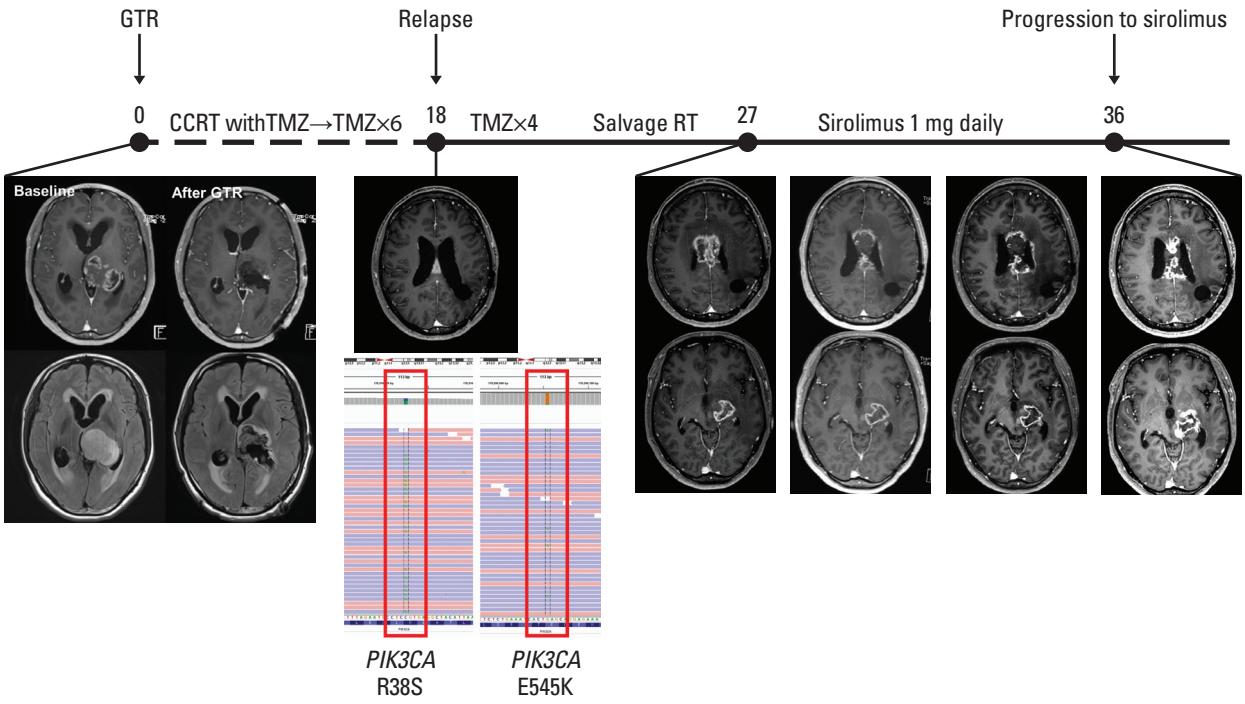

Fig. 4. History and images of patient DMG14 with *PIK3CA* mutation. Integrative genomics viewer, and MRI images of patient DMG14 with *PIK3CA* mutation who received sirolimus. The numbers above the timeline show months from the initiation of surgery. CCRT, concurrent chemoradiotherapy; GTR, gross total resection; MRI, magnetic resonance imaging; RT, radiotherapy; TMZ, temozolomide.

genomic alterations by NGS were not associated with PFS6 (S8 Table).

4. Efficacy and survival outcomes of salvage systemic therapies

Eleven patients had received salvage systemic therapies. The median OS from the initiation of systemic therapy was 8.3 months (95% CI, 6.1 to NA) in these patients. Six of these patients had surgical resection, and GTR was achieved in two patients. Bevacizumab was administered in seven patients as first-line salvage therapy after CCRT with TMZ, three of whom received irinotecan as combination.

The objective response rate, median PFS, and median OS after bevacizumab-based regimen were 28.6%, 1.6 months (95% CI, 1.4 to NA) (S9A Fig.), and 6.1 months (95% CI, 6.1 to NA), respectively. The two responders showed longer OS rates (19.9 and 11.2 months) (S9B Fig.).

Two patients received matched therapies in clinical trials: patient DMG14 with concurrent *PIK3CA* R38S (variant allele frequency [VAF] of 57.8%) and E545K (VAF of 7.2%) mutations had received sirolimus (NCT02688881); and patient DMG23 with *KRAS* G12A mutation (VAF 24.0%) had received pan-RAF plus MEK inhibitors. Patient DMG14 who experienced rapid progression before the administration of sirolimus showed stable disease to sirolimus with a PFS of 8.4 months (Fig. 4). Patient DMG23 showed a metabolic response to pan-RAF plus MEK inhibitors at 1 month along with metabolic improvement at the ipsilateral hemisphere, although she stopped investigational products because of a poor general condition, resulting in an OS of 5.6 months (S10 Fig.).

Discussion

Despite growing attention concerning pediatric DMG in various studies, the data on adult patients with DMG are only described in few studies [7,8]. Here, we described the demographics of adult DMG patients and clinical outcomes of definitive treatments and palliative systemic treatments. Our study demonstrated that patients may receive matched therapies based on genomic profiles, implying potential feasibility of individualized approach for rare population of adult DMG.

As a driver mutation for glioblastoma, *H3F3A* mutation was first discovered by whole-exome sequencing of pediatric glioblastoma samples [5]. *H3F3A* K27M mutation enhances neural stem cell self-renewal and cooperates with the activating platelet-derived growth factor receptor α mutant and Trp53 loss to accelerate the development of diffuse brain-

stem gliomas [29]. We showed that a high incidence of *TP53* mutation, which is consistent with several previous studies (Table 2) [4,5,7,27]. *H3F3A* gain-of-function mutation also inhibits PRC2 activity to alter epigenetic silencing and increase H3K27 acetylation [30]. Through these mechanisms, DMGs reprogram the methylation landscape and gene expression to harbor distinct genomic, methylation, and transcriptomic profiles from other glioblastomas [4,5,31]. The distinct features of DMG from other glioblastomas also include an extremely rare frequency of *IDH1/2* mutation [8,32], a finding that was also observed in our study. Although *H3F3A* G34V-mutant glioma is primarily located at the cerebral hemisphere [4], our DMG34 case with *H3F3A* G34V mutation showed a midline location and *TP53* mutation (S2 Fig.), similar to typical *H3F3A* K27M-mutant DMG cases.

We failed to demonstrate the prognostic significance of genomic profiles such as *ATRX* mutation, *CDKN2A* deletion, and *PTEN* loss. This finding might be attributable to the small number of patients in our study as well as the poor prognosis of DMG [3,4].

The clinical outcomes of our adult patients with DMG were compared with those of two previous studies of adult patients with DMG (Table 3) [8,28]. Although the resection rate including GTR (9.1%) was higher in our study, no survival differences were found between the studies [3]. These results could have been attributed to the midline location of DMGs and their infiltrative nature being difficult for surgeons to achieve complete resection. By contrast, the survival outcomes were associated with the sensitivity to radiotherapy defined as PFS6 after radiotherapy in our study. Patients without progression at 6 months after radiotherapy survived longer than those with progression at 6 months after radiotherapy, suggesting the important role of radiotherapy in adult patients with DMG.

Although patients who received palliative systemic treatments had a median OS of 8.3 months, a few responders seemed to have a prolonged OS. Additionally, two of 13 patients who had targeted NGS received matched therapies, including pan-RAF plus MEK inhibitors to target *KRAS* mutation and sirolimus to target *PIK3CA* mutation, suggesting the potential approach for precision medicine-based therapy. Regarding pathogenic *PIK3CA* mutations, previous study has demonstrated the potential efficacy of sirolimus in refractory solid cancers [33]. A recent high-throughput combination drug screening strategy identified the potential therapeutic combination of the multi-histone deacetylase inhibitor panobinostat and proteasome inhibitor marizomib against the preclinical DMG model [34]. In addition, inhibition of EZH2, an enzymatic subunit of polycomb repressive complex 2, reduced tumor growth in the *H3* K27M-mutant mouse model and patient-derived cell lines, suggesting an epigenetic modifier as a potential therapeutic target for *H3* K27M-mutant patients with DMG [35,36]. However, these preclinical therapeutic strategies should be validated in patients with treatment-refractory or relapsed DMG.

The limitations of our retrospective study include the small number of patients with adult DMG as well as limited number of targeted NGS. Therefore, genomic demographics and their clinical associations are not fully elucidated in this study. In addition, there seemed modest benefits of matched investigational drugs in two patients.

In conclusion, our study demonstrated that a progression-free survival at 6 months after radiotherapy significantly improved survival in adult patients with DMG while surgical extent did not improve survival, suggesting the important role of radiotherapy in patients with adult brain DMG. Additionally, targeted sequencing revealed a high frequency of concurrent *TP53* mutation in combination with *H3F3A* or *HIST1H3B* mutation. Considering two patients with MAPK-*PI3K* alterations received matched therapy, a precision medicine-guided treatment approach might be feasible in adult patients with brain DMG. Future efforts should be directed toward targeting histone/chromatin modification or co-targeting histone/chromatin modification and other pathways based on the DMG genome in a basket or platform trial.

Electronic Supplementary Material

Supplementary materials are available at Cancer Research and Treatment website (https://www.e-crt.org).

Ethical Statement

All of data collection and analysis were performed after approval from the institutional review board (IRB No. 1811-054-983) in accordance with the declaration of Helsinki. The written informed consent was waived in this retrospective study.

Author Contributions

Conceived and designed the analysis: Park C, Kim TM.
Collected the data: Park C, Kim TM, Bae JM, Yun H, Kim JW, Choi SH, Lee ST, Lee JH, Park SH, Park CK.
Contributed data or analysis tools: Park C, Kim TM, Bae JM, Yun H, Kim JW, Choi SH, Lee ST, Lee JH, Park SH, Park CK.
Performed the analysis: Park C, Kim TM, Yun H.
Wrote the paper: Park C, Kim TM, Bae JM, Yun H, Kim JW, Choi SH, Lee ST, Lee JH, Park SH, Park CK.

Conflicts of Interest

Dr. Tae Min Kim received grants from AstraZeneca-KHIDI outside this work. The other authors declare no potential conflicts of interest.

Acknowledgments

This study was supported by a grant from the Korean Health Technology R&D Project "Strategic Center of Cell and Bio Therapy for Heart, Diabetes & Cancer" through the Korea Health Industry Development Institute (KHIDI) funded by the Ministry of Health & Welfare (MHW) (grant number: HI-17C-2085, T.M.K.).

We thank Juyoun Kim who managed the database, the neuro-oncology multidisciplinary team at SNUH, and patients and their families.

References

1. Louis DN, Perry A, Reifenberger G, von Deimling A, Figarella-Branger D, Cavenee WK, et al. The 2016 World Health Organization classification of tumors of the central nervous system: a summary. Acta Neuropathol. 2016;131:803-20.
2. Gielen GH, Gessi M, Hammes J, Kramm CM, Waha A, Pietsch T. H3F3A K27M mutation in pediatric CNS tumors: a marker for diffuse high-grade astrocytomas. Am J Clin Pathol. 2013;139:345-9.
3. Karremann M, Gielen GH, Hoffmann M, Wiese M, Colditz N, Warmuth-Metz M, et al. Diffuse high-grade gliomas with H3 K27M mutations carry a dismal prognosis independent of tumor location. Neuro Oncol. 2018;20:123-31.
4. Mackay A, Burford A, Carvalho D, Izquierdo E, Fazal-Salom J, Taylor KR, et al. Integrated molecular meta-analysis of 1,000 pediatric high-grade and diffuse intrinsic pontine glioma. Cancer Cell. 2017;32:520-37.
5. Schwartzentruber J, Korshunov A, Liu XY, Jones DT, Pfaff E, Jacob K, et al. Driver mutations in histone H3.3 and chromatin remodelling genes in paediatric glioblastoma. Nature. 2012;482:226-31.
6. Buczkowicz P, Hoeman C, Rakopoulos P, Pajovic S, Letourneau L, Dzamba M, et al. Genomic analysis of diffuse intrinsic pontine gliomas identifies three molecular subgroups and recurrent activating ACVR1 mutations. Nat Genet. 2014;46:451-6.
7. Aihara K, Mukasa A, Gotoh K, Saito K, Nagae G, Tsuji S, et al. H3F3A K27M mutations in thalamic gliomas from young adult patients. Neuro Oncol. 2014;16:140-6.
8. Meyronet D, Esteban-Mader M, Bonnet C, Joly MO, Uro-Coste E, Amiel-Benouaich A, et al. Characteristics of H3 K27M-mutant gliomas in adults. Neuro Oncol. 2017;19:1127-34.
9. Rodon J, Soria JC, Berger R, Miller WH, Rubin E, Kugel A, et al. Genomic and transcriptomic profiling expands precision cancer medicine: the WINTHER trial. Nat Med. 2019;25:751-8.
10. Stupp R, Mason WP, van den Bent MJ, Weller M, Fisher B, Taphoorn MJ, et al. Radiotherapy plus concomitant and adjuvant temozolomide for glioblastoma. N Engl J Med. 2005;352:987-96.
11. Sulman EP, Ismaila N, Armstrong TS, Tsien C, Batchelor TT, Cloughesy T, et al. Radiation therapy for glioblastoma: American Society of Clinical Oncology clinical practice guideline endorsement of the American Society for Radiation Oncology guideline. J Clin Oncol. 2017;35:361-9.
12. Wen PY, Macdonald DR, Reardon DA, Cloughesy TF, Sorensen AG, Galanis E, et al. Updated response assessment criteria for high-grade gliomas: response assessment in neuro-oncology working group. J Clin Oncol. 2010;28:1963-72.
13. Ballman KV, Buckner JC, Brown PD, Giannini C, Flynn PJ, LaPlant BR, et al. The relationship between six-month progression-free survival and 12-month overall survival end points for phase II trials in patients with glioblastoma multiforme. Neuro Oncol. 2007;9:29-38.
14. Li H. Exploring single-sample SNP and INDEL calling with whole-genome de novo assembly. Bioinformatics. 2012;28:1838-44.
15. Van der Auwera GA, Carneiro MO, Hartl C, Poplin R, Del Angel G, Levy-Moonshine A, et al. From FastQ data to high confidence variant calls: the Genome Analysis Toolkit best practices pipeline. Curr Protoc Bioinformatics. 2013;43:11.10.1-33.
16. Wilm A, Aw PP, Bertrand D, Yeo GH, Ong SH, Wong CH, et al. LoFreq: a sequence-quality aware, ultra-sensitive variant caller for uncovering cell-population heterogeneity from high-throughput sequencing datasets. Nucleic Acids Res. 2012;40:11189-201.
17. Rausch T, Zichner T, Schlattl A, Stutz AM, Benes V, Korbel JO. DELLY: structural variant discovery by integrated paired-end and split-read analysis. Bioinformatics. 2012;28:i333-9.
18. Chen X, Schulz-Trieglaff O, Shaw R, Barnes B, Schlesinger F, Kallberg M, et al. Manta: rapid detection of structural variants and indels for germline and cancer sequencing applications. Bioinformatics. 2016;32:1220-2.
19. Oesper L, Satas G, Raphael BJ. Quantifying tumor heterogeneity in whole-genome and whole-exome sequencing data. Bioinformatics. 2014;30:3532-40.
20. Talevich E, Shain AH, Botton T, Bastian BC. CNVkit: genome-wide copy number detection and visualization from targeted DNA sequencing. PLoS Comput Biol. 2016;12:e1004873.
21. Cingolani P, Platts A, Wang le L, Coon M, Nguyen T, Wang L, et al. A program for annotating and predicting the effects of single nucleotide polymorphisms, SnpEff: SNPs in the genome of Drosophila melanogaster strain w1118; iso-2; iso-3. Fly (Austin). 2012;6:80-92.
22. O'Leary NA, Wright MW, Brister JR, Ciufo S, Haddad D, McVeigh R, et al. Reference sequence (RefSeq) database at NCBI: current status, taxonomic expansion, and functional annotation. Nucleic Acids Res. 2016;44:D733-45.
23. Tate JG, Bamford S, Jubb HC, Sondka Z, Beare DM, Bindal N, et al. COSMIC: the Catalogue Of Somatic Mutations In Cancer. Nucleic Acids Res. 2019;47:D941-7.

24. Sherry ST, Ward MH, Kholodov M, Baker J, Phan L, Smigielski EM, et al. dbSNP: the NCBI database of genetic variation. Nucleic Acids Res. 2001;29:308-11.
25. Landrum MJ, Lee JM, Riley GR, Jang W, Rubinstein WS, Church DM, et al. ClinVar: public archive of relationships among sequence variation and human phenotype. Nucleic Acids Res. 2014;42:D980-5.
26. Lek M, Karczewski KJ, Minikel EV, Samocha KE, Banks E, Fennell T, et al. Analysis of protein-coding genetic variation in 60,706 humans. Nature. 2016;536:285-91.
27. Nikbakht H, Panditharatna E, Mikael LG, Li R, Gayden T, Osmond M, et al. Spatial and temporal homogeneity of driver mutations in diffuse intrinsic pontine glioma. Nat Commun. 2016;7:11185.
28. Schreck KC, Ranjan S, Skorupan N, Bettegowda C, Eberhart CG, Ames HM, et al. Incidence and clinicopathologic features of H3 K27M mutations in adults with radiographically-determined midline gliomas. J Neurooncol. 2019;143:87-93.
29. Larson JD, Kasper LH, Paugh BS, Jin H, Wu G, Kwon CH, et al. Histone H3.3 K27M accelerates spontaneous brainstem glioma and drives restricted changes in bivalent gene expression. Cancer Cell. 2019;35:140-55.
30. Lewis PW, Muller MM, Koletsky MS, Cordero F, Lin S, Banaszynski LA, et al. Inhibition of PRC2 activity by a gain-of-function H3 mutation found in pediatric glioblastoma. Science. 2013;340:857-61.
31. Chan KM, Fang D, Gan H, Hashizume R, Yu C, Schroeder M, et al. The histone H3.3K27M mutation in pediatric glioma reprograms H3K27 methylation and gene expression. Genes Dev. 2013;27:985-90.
32. Sturm D, Witt H, Hovestadt V, Khuong-Quang DA, Jones DT, Konermann C, et al. Hotspot mutations in H3F3A and IDH1 define distinct epigenetic and biological subgroups of glioblastoma. Cancer Cell. 2012;22:425-37.
33. Jung KS, Lee J, Park SH, Park JO, Park YS, Lim HY, et al. Pilot study of sirolimus in patients with PIK3CA mutant/amplified refractory solid cancer. Mol Clin Oncol. 2017;7:27-31.
34. Lin GL, Wilson KM, Ceribelli M, Stanton BZ, Woo PJ, Kreimer S, et al. Therapeutic strategies for diffuse midline glioma from high-throughput combination drug screening. Sci Transl Med. 2019;11:eaaw0064.
35. Yamaguchi H, Hung MC. Regulation and role of EZH2 in cancer. Cancer Res Treat. 2014;46:209-22.
36. Mohammad F, Weissmann S, Leblanc B, Pandey DP, Hojfeldt JW, Comet I, et al. EZH2 is a potential therapeutic target for H3K27M-mutant pediatric gliomas. Nat Med. 2017;23:483-92.